

Small-scale turbulent dynamo for low-Prandtl number fluid: comparison of the theory with results of numerical simulations.

A.V. Kopyev¹, A.S. Il'yn^{1,2}, V.A. Sirota¹, and K.P. Zybin^{1,2}

¹ P.N.Lebedev Physical Institute of RAS, 119991, Leninskij pr.53, Moscow, Russia

² National Research University Higher School of Economics, 101000, Myasnitskaya 20, Moscow, Russia

December 29, 2025

ABSTRACT

Context. During the last decades, significant progress has been made in both numerical simulations of turbulent dynamo and theoretical understanding of turbulence. However, there is still lack of quantitative comparison between the simulations and the theory of the dynamo.

Aims. Our aim is to investigate generation of magnetic field by the incompressible turbulent conductive fluid near the critical regime and compare theoretical predictions of Kazantsev model with results of recent direct numerical simulations.

Methods. The Kazantsev equation is analyzed both analytically and numerically.

Results. We study the critical magnetic Reynolds number (Rm_c) and the growth rate near the threshold both in the limit of very high and in the case of moderate Reynolds numbers. We argue that in Kazantsev equation for magnetic field generation, one should use the quasi-Lagrangian correlator of velocities instead of Eulerian, as usually implied when comparing theory and simulations. The theoretical results obtained with this correlator agree well with numerical results. We also propose the explanation of the decrease of Rm_c as a function of Reynolds number (Re) at intermediate-high Re . It is probably due to Reynolds-dependent intermittency of the velocity structure function: we show that the scaling exponent of this function in the inertial range affects strongly the magnetic field generation, and it is known to be an increasing function of the Reynolds number.

Conclusions. Use of quasi-Lagrangian correlator in the Kazantsev theory gives good accordance with numerical simulations. An ideal way to compare them should be to find the correlator substituted to the Kazantsev equation and the generation properties in the same simulation. At least one has to use universal parameters independent of the properties of pumping scale. Reynolds-dependent intermittency can explain recently observed decrease of the critical magnetic Reynolds number at small Prandtl numbers.

Key words. Dynamo – magnetohydrodynamics (MHD) – turbulence – Sun: magnetic fields

1. Introduction

The theory of how magnetic fields arise in turbulent flows of conductive fluid has wide applications, particularly in explaining the magnetic fields observed in many astrophysical objects (see, e.g., Brandenburg & Subramanian 2005; Jouve et al. 2008; Moss et al. 2013; Brandenburg et al. 2024). The case of small-scale magnetic field, i.e., the field with characteristic scale much smaller than the integral scale of turbulence, has been studied in numerous papers (see, e.g., Zeldovich et al. 1990; Falkovich et al. 2001; Brandenburg et al. 2012). Conductive fluids can be classified by their magnetic Prandtl number,

$$Pm = \nu/\eta \quad (1)$$

where ν is viscosity and η is magnetic diffusivity. In the case $Pm \gg 1$, the resistive scale lies deep inside the viscous range of turbulence (Batchelor 1950; Zel'dovich et al. 1984; Chertkov et al. 1999). In this paper we concentrate on the other case of fluids with low and intermediate Pm : this means that the resistive scale is larger than the viscous scale, so, excitation of magnetic fluctuations is driven by the inertial-range or 'bottleneck' velocity fluctuations.

Theoretical description of the process in the incompressible fluid is based on the Kazantsev equation, which relates the evolution of the magnetic field pair correlator and the velocity structure

function. Experimental possibilities are rather limited in terrestrial conditions. Direct numerical simulations (DNS) of low Pm , unlike the case of large Prandtl numbers, face difficulties in modeling magnetic field advection in the inertial range of turbulence and demonstrate some discrepancies between different simulations (see, e.g., Warnecke et al. 2023, Fig.2).

However, during the last decades, significant progress has been made in both theoretical understanding of the properties of turbulence (L'vov et al. 1997; Donzis & Sreenivasan 2010; Biferale et al. 2011; Iyer et al. 2020) and the environment and technics of DNS (Iskakov et al. 2007; Schekochihin et al. 2007; Brandenburg et al. 2018; Warnecke et al. 2023; Rempel et al. 2023), which has resulted in high resolution and advanced to lower values of Pm . This progress gives hope to proceed from qualitative correspondence to more or less thorough quantitative comparison at least between theory and DNS.

In study of turbulence, after the theoretical model formulation (for decaying turbulence) in the classical work (Kolmogorov 1941) and its development for stationary turbulence (Novikov 1965), precision testing of the results of the model was performed in experiments (Moisy et al. 1999). The coincidence of theoretical predictions and experimental measurements has, citing Moisy et al. (1999), demonstrated 'the relevance of isotropic homogeneous turbulence state approximation, used in almost all theoretical approaches to turbulence'. For low- Pm dynamo such program seems hardly possible because of experimental difficul-

ties. However, in absence of experimental approbation, accurate quantitative comparison with DNS becomes even more important. It could validate both of the approaches: it would verify the resolution of DNS, and check the applicability of theoretical assumptions of delta- time correlation (Tobias et al. 2012) and Gaussianity of the turbulent velocity field. It could also test non-trivial effects resulting from non-Gaussianity, e.g., weakening of magnetic field generation and corrections to the magnetic energy spectrum (Kopyev et al. 2022a,b, 2024). Finally, if the theory were confirmed for moderate-low magnetic Prandtl numbers, one could scale it to extremely low Pm , unattainable by current facilities and typical for astrophysical objects.

Correct interpretation of numerical data on velocity correlators for their comparison with the theory is one of the problems on this path. In the Kazantsev theory, velocity correlators are assumed to be δ -correlated in time, and the velocity distribution acts in Kazantsev equation by means of the multiplier $b(\rho)$ in the structure function,

$$\langle \delta v_{\parallel}(\rho, t) \delta v_{\parallel}(\rho, t') \rangle_{Kaz} = 2b(\rho) \delta(t - t'), \quad (2)$$

where longitudinal velocity increments in two near points are

$$\delta v_{\parallel}(\rho, t) = (v(\mathbf{r} + \rho, t) - v(\mathbf{r}, t)) \frac{\rho}{\rho} \quad (3)$$

The correlator is independent of t , \mathbf{r} and of the direction of ρ , because of homogeneity and isotropy of turbulence.

To restore the amplitude $b(\rho)$ from given correlator, one can use the expression (Vainshtein 1980; Kichatinov 1985)

$$b(\rho) = \frac{1}{2} \int_{-\infty}^{\infty} d\tau \langle \delta v_{\parallel}(\rho, \tau) \delta v_{\parallel}(\rho, 0) \rangle \quad (4)$$

For δ -correlated process there is no difference whether one calculates δv_{\parallel} at a fixed point \mathbf{r} of space, or at the point $\mathbf{r}(t)$ moving arbitrarily; the correlator is the same. One also obtains the same result for quasi-Lagrangian reference frame, i.e., $\mathbf{r}(t)$ tracing one arbitrary fluid particle (L'vov et al. 1997). This frame is distinguished, e.g., by the fact that the Kazantsev predictions must be consistent with the results obtained from 'evolutionary' approach (Zel'dovich et al. 1984; Chertkov et al. 1999), wherever both of the models are applicable; and the evolutionary approach explicitly considers the quasi-Lagrangian frame.

In 'real' turbulent flows, including those in DNS, all structure functions have non-zero correlation time, and the values of $b(\rho)$ calculated in different frames (i.e., for different $\mathbf{r}(t)$ in (3)) differ essentially. The analysis of data from John Hopkins database shows that at high Reynolds numbers, for all scales $\langle \delta v_{\parallel}(\rho, \tau) \delta v_{\parallel}(\rho, 0) \rangle^{Eul} \propto 1/\tau$ (Kopyev et al. 2026). If so, the logarithmic divergence of (4) corresponds to the growth of magnetic field faster than exponential; this would contradict to the Oseledets theorem (Oseledec 1968). We note that, unlike the Eulerian case, the quasi-Lagrangian $b(\rho)$ converges well: $\langle \delta v_{\parallel}(\rho, \tau) \delta v_{\parallel}(\rho, 0) \rangle^{Lagr}$ decays exponentially with respect to τ (Biferale et al. 2011).

Consider now some experiment or simulation. Which $b(\rho)$ should we substitute to the Kazantsev equation in order to compare the theory results with the experiment? In other words, which $b(\rho)$ 'simulates' the correct amplitude for the effective δ -correlator? The choice of the Eulerian frame ($\mathbf{r} = \text{const}$) in (3), though may seem most natural, is in fact not preferable, and probably is just incorrect. Maybe it was the reason that prevented Mason et al. (2011) from getting a good correspondence

between theory and DNS. Consistent solution to the problem must be based on accurate dynamical analysis and is far from being performed yet. But we suppose that the correct answer is to choose the quasi-Lagrangian frame. The grounds for this supposition are as follows:

- First, from the renewing model (Zel'dovich et al. 1984) it follows (Zeldovich et al. 1990; Rogachevskii & Kleeorin 1997) that if the correlation time is smaller than all other characteristic timescales, the quasi-Lagrangian frame gives the correct result: the Kazantsev approach can be in this case verified by 'evolutionary' models. Actually, this is the case near the generation threshold: the characteristic time for magnetic field evolution is large, so the delta approximation for velocity correlations works well.

- Second, for arbitrary correlation time but only for large magnetic Prandtl numbers (which restricts the consideration to the viscous range of scales), the choice of the quasi-Lagrangian frame is also correct (Vainshtein 1980; Kichatinov 1985). Recently, Il'yn et al. (2022) have shown the quasi-Lagrangian correlators to be equivalent to effective δ -correlators in long-time approximation.

By analogy with the limit cases, it is reasonable to imply the quasi-Lagrangian velocity increments in (3), (4). The relevance of this assumption will be validated in this paper by means of direct comparison of the predictions of the theory based on the Kaznatsev equation with the velocity structure function $b(\rho)$ determined in this way with the results of DNS. The good compliance is the proof of our choice of the quasi-Lagrangian structure function.

In this paper we calculate the critical magnetic Reynolds number and the increments of the magnetic field correlator near the critical regime of generation. To this purpose, we solve the Kazantsev equation with quasi-Lagrangian velocity structure function (4). Basic notations and equations are introduced in Section 2. Unfortunately, there is not much data on quasi-Lagrangian velocity structure functions. So, we consider two different cases: the Taylor Reynolds number $Re_{\lambda} = 140$ (Section 3), the one for which there is DNS data on both magnetic field (Schekochihin et al. 2007) and velocity correlators (Biferale et al. 2011; Donzis & Sreenivasan 2010), and the limit of infinite Reynolds number (Section 4) where the shape of the velocity correlator is chosen based on theoretical reasons. For this case, we use different approximations and consider the effects produced by the declination of the velocity structure function exponent from the Kolmogorov scaling in the inertial range of turbulence (L'vov et al. 1997; Iyer et al. 2020) and the properties of the transition range between the inertial and largest-eddy scales. We compare the results with the numerical data Iskakov et al. (2007); Schekochihin et al. (2007); Brandenburg et al. (2018); Warnecke et al. (2023) and find quite good correspondence. We also show that the Reynolds-dependent intermittency of velocity structure functions (Iyer et al. 2020) can explain the observed decrease of the critical Reynolds number at small Prandtl numbers (Warnecke et al. 2023).

We calculate the magnetic field correlator's growth rate in the vicinity of the generation threshold and compare the results with the DNS (Section 5).

Finally, in Discussion we summarize the results of the paper and comment on further prospects and possible improvements in comparison of the Kazantsev theory predictions with experiments and simulations. In particular, we point to the properties of quasi-Lagrangian turbulence that could be found from DNS

together with the magnetic generation properties, to make the comparison with the theory quantitative (not only qualitative) and precise.

2. Basic equations and parameters

The evolution of the magnetic field $\mathbf{B}(\mathbf{r}, t)$ is governed by the induction equation

$$\frac{\partial \mathbf{B}(\mathbf{r}, t)}{\partial t} = \nabla \times [\mathbf{v}(\mathbf{r}, t) \times \mathbf{B}(\mathbf{r}, t)] + \eta \nabla^2 \mathbf{B}(\mathbf{r}, t). \quad (5)$$

Since the back-reaction of the magnetic field on the flow is quadratic in field strength and the initial (seed) magnetic field is weak, we can neglect its influence on the velocity dynamics. In this kinematic regime, the magnetic field acts as a passive vector field advected by the flow. The solenoidal velocity field $\mathbf{v}(\mathbf{r}, t)$ is treated as a prescribed stochastic field with stationary statistics. The correlation function of the magnetic field

$$G(\rho, t) = \langle B_{\parallel}(\mathbf{r} + \boldsymbol{\rho}, t) B_{\parallel}(\mathbf{r}, t) \rangle, \quad B_{\parallel} = \mathbf{B} \cdot \boldsymbol{\rho} / \rho \quad (6)$$

is assumed to be independent of \mathbf{r} in homogenous isotropic flow. Its evolution under assumption (2) is described by the equation (Kazantsev 1968)

$$\frac{\partial}{\partial t} G(\rho, t) = 2S(\rho) \left(G''_{\rho\rho} + \frac{4G'_{\rho}}{\rho} \right) + 2S'G'_{\rho} + 2 \left(S'' + 4\frac{S'}{\rho} \right) G \quad (7)$$

where

$$S(\rho) = \eta + \frac{1}{2}b(\rho),$$

and the function $b(\rho)$ is defined in (4). We are interested in exponential behavior of magnetic field, so we look for a solution in the form

$$G = e^{\gamma t} \psi(\rho) / (\rho^2 \sqrt{S})$$

Then ψ satisfies the Schrodinger type equation (Kazantsev 1968)

$$\psi''_{\rho\rho} = \frac{\gamma}{2S(\rho)} \psi + U(\rho) \psi, \quad (8)$$

$$U = -\frac{1}{\rho^2} \left(\frac{3\sigma(\sigma+4)+1}{4} + \frac{\rho\sigma'}{2} \right), \quad (9)$$

$$\sigma(\rho) = \frac{d \ln S}{d \ln \rho} - 1 \quad (10)$$

with the boundary condition $\psi(0) = 0$, $\psi(\infty) < \infty$. We solve this equation numerically by means of a modification of the stochastic quantization idea (Il'yn et al. 2021, Appendix A).

To compare the theory with the results of DNS, one has to normalize the dimensional parameters. Generally, isotropic hydrodynamical flow is completely characterized by three dimensional parameters (Novikov 1965; Moisy et al. 1999):

$$\nu, \quad \varepsilon = \nu \left\langle \frac{\partial v_i}{\partial x_k} \frac{\partial v_i}{\partial x_k} \right\rangle, \quad u' = \sqrt{\langle v_i v_i \rangle / 3} = v_{rms} / \sqrt{3}$$

where ν is viscosity, ε is the total energy flux from larger to smaller scales, v_{rms} is the volume integrated root-mean-squared velocity. From these three parameters one can compose one universal dimensionless combination, e.g.,

$$Re_{\lambda} \equiv \frac{u' \lambda}{\nu} = \frac{\sqrt{15} u'^2}{\sqrt{\varepsilon \nu}}, \quad (11)$$

where $\lambda = u' \sqrt{15\nu/\varepsilon}$ is the Taylor scale; this parameter is called the Taylor Reynolds number. However, 'classical' Reynolds number is often used,

$$Re = v_{rms} L / \nu$$

where L is the pumping scale, or the largest eddies scale, and is not defined universally. This uncertainty produces difficulties in matching different experimental/DNS results and their comparison with the theory. (For example, Brandenburg et al. (2018) reported some obstacles when comparing their results with Schekochihin et al. (2007)). Here we define

$$Re^{(Sch)} = \frac{Re_{\lambda}^2}{30} = \frac{u'^4}{2\varepsilon\nu} \quad (12)$$

This corresponds to relations between Re and Re_{λ} used by Schekochihin et al. (2007).

The magnetic properties of the fluid can be described by the dimensionless magnetic Prandtl number (1). The magnetic Reynolds number

$$Rm = Pm \cdot Re \quad (13)$$

is also generally used. Unlike Pm , it depends on the choice of L in the definition of the Reynolds number.

So, we are interested in the stability condition $Pm_c(Re_{\lambda})$, or $Rm_c(Re)$ such that there is a solution of (8) with $\gamma = 0$ and there is no solution with $\gamma > 0$ for smaller Rm . We note that the second relation is conventional, but the first one is more universally defined.

In the vicinity of this stability curve, γ is known to depend log-linearly on Rm (Rogachevskii & Kleerorin 1997; Kleerorin & Rogachevskii 2012):

$$\gamma \propto \ln(Rm/Rm_c).$$

Based on Eq. (8), we calculate the proportionality coefficient numerically and compare it with the results of Warnecke et al. (2023).

To solve Eq. (8), one has to assume some model for $b(\rho)$. This produces one more difficulty, since $b(\rho)$ is the quasi Lagrangian correlation function, and is difficult to measure (Biferale et al. 2011). By definition of the Lagrangian correlation time $\tau_c(\rho)$ introduced by L'vov et al. (1997), we have:

$$b(\rho) = \langle (\delta v_{\parallel})^2 \rangle(\rho) \tau_c(\rho) \quad (14)$$

In Biferale et al. (2011); Donzis & Sreenivasan (2010) the simultaneous structure function $\langle (\delta v_{\parallel})^2 \rangle$ and the correlation time τ_c are found from DNS for $Re_{\lambda} = 140$; for much higher Re_{λ} we make use of theoretical considerations (L'vov et al. 1997) that argue that both $\langle (\delta v_{\parallel})^2 \rangle$ and τ_c are power law functions of ρ inside the inertial range.

3. $Re_{\lambda} = 140$: moderate Re and Pm

In this section we base on the results of Biferale et al. (2011); Donzis & Sreenivasan (2010) for data on velocity statistics and Iskakov et al. (2007); Schekochihin et al. (2007) for data on magnetic generation. Fortunately, all these papers contain the DNS performed for the same Reynolds number $Re_{\lambda} = 140$. The critical Prandtl number is not small for this Reynolds number, so the bottleneck region and even the viscous range of scales may affect the results and have to be taken into account. The main parameters of the DNS performed by Biferale et al. (2011) are listed in Table 1.

Table 1. Main parameters of the flow in the paper of Biferale et al. (2011)

Parameter	Value
Integral scale	$L = 4.24$
Taylor scale	$\lambda = 0.30$
Kolmogorov viscous scale	$r_v = 1.28 \times 10^{-2}$
Energy flux	$\varepsilon = 1$
Kinematic viscosity	$\nu = 3 \times 10^{-3}$
Single-component RMS velocity	$u' = 1.41$

Biferale et al. (2011) calculate the dependence of Lagrangian correlation time τ_c on ρ :

$$\tau_c(\rho) = C_1 t_v \frac{(1 + (C_2 \rho / r_v)^2)^{1/3}}{(1 + (C_3 \rho / L)^2)^{1/3}} \quad (15)$$

where

$$C_1 = 2.15, \quad C_2 = 6.75 \cdot 10^{-2}, \quad C_3 = 2.94,$$

$r_v = \nu^{3/4} \varepsilon^{-1/4}$ is the Kolmogorov viscous scale, and $t_v = \sqrt{\nu / \varepsilon}$ is the viscous characteristic time.

The second-order simultaneous velocity structure function is well investigated; in the viscous and inertial ranges its behavior is universal and is very well described by the generalized Batchelor approximation (Donzis & Sreenivasan 2010):

$$\langle (\delta v_{\parallel})^2 \rangle = \frac{\varepsilon}{15\nu} \frac{\rho^2}{\left(1 + (C_B \rho / r_v)^q\right)^{\frac{2-\zeta_2}{q}}}, \quad \rho \ll L, \quad (16)$$

$$C_B = 7.6 \times 10^{-2}, \quad \zeta_2 = 0.67, \quad q = 1.82$$

It is easy to see that in the 'ultraviolet' regime it coincides with Kolmogorov's analytical formula, $\langle (\delta v_{\parallel})^2 \rangle = \frac{\varepsilon}{15\nu} \rho^2$, $\rho \ll r_v$, while inside the inertial range it demonstrates power-law behavior, $\langle (\delta v_{\parallel})^2 \rangle \propto \rho^{\zeta_2}$, $L \gg \rho \gg r_v / C_B$. We note that both coefficients C_B in (16) and C_2 in (15) are comparably small. This corresponds to the existence of the bottleneck transition region between the viscous and the inertial ranges: viscosity is essential at scales $\rho \sim r_v / C_2 \simeq r_v / C_B$ significantly larger than the viscous scale.

For our purpose, we have to enlarge the limits of applicability of (16) for larger scales up to the integral scale, where $\langle (\delta v_{\parallel})^2 \rangle = 2u'^2$, $\rho \geq L$. In accordance with the ideology of extended self-similarity (ESS), this can also be done by means of fractionally rational approximation¹:

$$\langle (\delta v_{\parallel})^2 \rangle_{(main)} = \frac{\varepsilon}{15\nu} \frac{\rho^2}{\left(1 + (C_B \rho / r_v)^q\right)^{\frac{2-\zeta_2}{q}} \left(1 + (C_m \rho / L)^2\right)^{\frac{\zeta_2}{2}}}, \quad (17)$$

where $C_m = 1.6$ follows from the matching with the integral scale.

The two transitional regions, the bottleneck and the range between the inertial and integral scales, are presented in (17) by

¹ For this shape of the correlation functions,

$$\frac{\zeta_2(r)}{\zeta_3(r)} \equiv \frac{d \ln \langle (\delta v_{\parallel})^2 \rangle}{d \ln \langle |\delta v_{\parallel}|^3 \rangle} = const$$

in accordance with ESS (Benzi et al. 1993).

Table 2. Critical magnetic Prandtl numbers and magnetic Reynolds numbers at $Re_{\lambda} = 140$ for different theoretical models and DNS

$Re_{\lambda} = 140$	Approx.	Pm_c	Rm_c^{sch}
Main model	(15), (17)	0.26	170
Sharp sub-integral transition	(15), (18)	0.22	140
Sharp bottleneck	(15), (19)	0.29	190
DNS (Schekochihin et al. 2007)	—	0.3	195

the two brackets in the denominator. To estimate the accuracy of the approximation and to visualize the contributions of the two transition regions, we consecutively substitute a piecewise-power law function for each of the brackets

$$\langle (\delta v_{\parallel})^2 \rangle_{(sharp-int)} = \frac{\varepsilon}{15\nu} \frac{\rho^2}{\left(1 + (C_B \rho / r_v)^q\right)^{\frac{2-\zeta_2}{q}}} \theta(L/a_{int} - \rho) + 2u' \theta(\rho - L/a_{int}) \quad (18)$$

and

$$\langle (\delta v_{\parallel})^2 \rangle_{(sharp-bot)} = \frac{\varepsilon}{15\nu} \frac{\rho^2}{\left(1 + (C_m \rho / L)^2\right)^{\frac{\zeta_2}{2}}} \theta(\rho - a_{bot} r_v) + \frac{\varepsilon}{15\nu} \rho^2 \theta(a_{bot} r_v - \rho), \quad (19)$$

The coefficients $a_{bot} = 13.1$ and $a_{int} = 1.6$ are also found from the matching condition, as well as C_B and C_m . The value of a_{int} coincides to high accuracy with C_m , which indicates that the two approximations are rather close.

The results are presented in Table 2. One can see that the predictions of the theory are rather close to the numerical results; the use of the Eulerian structure function $b(\rho)$ would give the estimate of Rm_c at least an order of magnitude less.

The fact that the theoretical prediction for Rm_c is lower than the experimental result may be caused by the assumption of Gaussianity of the flow: taking into account the declination from Gaussianity, i.e., the third order correlator of velocity, can increase the result (Kopyev et al. 2024).

The critical values of the magnetic Reynolds number and Prandtl number are close for all the three models; however, the results still differ to about 15%. This indicates the influence of the transitional regions on the near-threshold generation. The importance of the bottleneck region is determined by the fact that the magnetic Prandtl number is not small enough to neglect the influence of the viscous range. Indeed, from the value of C_B in (17) and C_2 in (15) it follows that the influence of the viscosity reaches about $15r_v$, while for $Pm = 0.25$ the magnetic diffusivity scale is only about $3r_v$, so it lies deep inside the bottleneck range. It is natural to suppose that for smaller Pm , the effect of viscosity on the magnetic field generation decreases. Oppositely, the influence of the 'external' transition between the inertial and the integral ranges can only become even more important for larger Reynolds numbers.

4. Very large Reynolds numbers

Lack of experimental or DNS data on hydrodynamic Lagrangian correlation time does not allow us to find $b(\rho)$ for other Reynolds numbers, and, hence, to calculate Rm_c for them. However, for

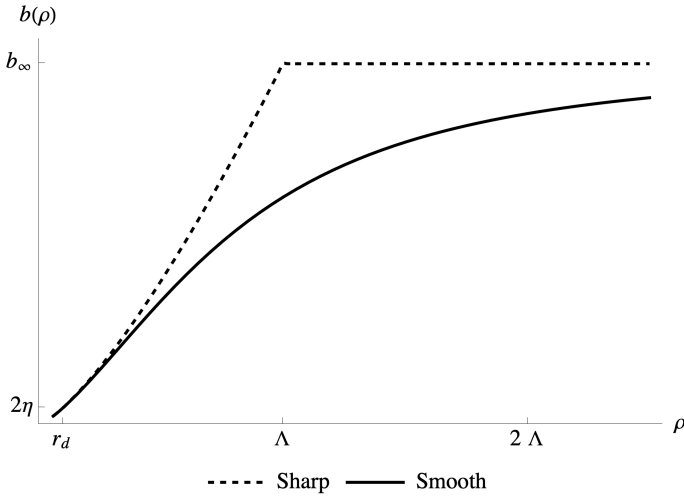


Fig. 1. Shape of $b(\rho)$ for the Sharp (Eq. 26) and the Smooth (Eq. 28) models, for the same values of the parameters s , b_∞ and Λ .

well developed turbulence with wide inertial range one can, in accordance with general theoretical approach to turbulence, suppose that $b(\rho)$ has universal shape independent of the details of the flow. To normalize the function, one has to take the largest scales. For these scales,

$$\lim_{\rho \rightarrow \infty} \langle (\delta v_\parallel)^2 \rangle = \frac{2}{3} v_{rms}^2 = 2u'^2 \quad (20)$$

and the integral Lagrangian correlation time $T_L = \lim_{\rho \rightarrow \infty} \tau_c$ can be found from the approximation based on Sawford's second-order stochastic model (Sawford 1991; Sawford et al. 2008):

$$T_L = \sqrt{\frac{\nu}{\varepsilon}} \frac{2Re_\lambda}{\sqrt{15}C_0} = \frac{2}{C_0} \frac{u'^2}{\varepsilon} \quad (21)$$

where C_0 is the Kolmogorov constant. It is rather difficult to find (Lien & D'Asaro 2002; Ouellette et al. 2006; Zimmermann et al. 2010), here we use the value obtained by Sawford & Yeung (2011):

$$C_0 = 6.9 \pm 0.2. \quad (22)$$

So, in what follows, we consider different models for $b(\rho)$ that satisfy the normalization condition consistent with (14):

$$b_\infty \equiv b(\infty) = 2u'^2 T_L \quad (23)$$

According to (21), (11), (1),

$$\frac{b_\infty}{2\eta} = Pm \frac{Re_\lambda^2}{15} \frac{2}{C_0} \propto Rm \quad (24)$$

In what follows, we use the dimensionless value

$$X = \left(\frac{b_\infty}{2\eta} \right)^{1/(1+s)} \quad (25)$$

to characterize the generation properties of a flow. Here s is the scaling exponent of $\langle |\delta v_\parallel| \rangle$. The value of X describes the relative width of the range of scales that can affect the generation. We note that for any particular series of DNS or experiments, $Rm \propto X^{1+s}$, however, because of uncertainty of the definition of the integral scale L , X is more accurately defined than Rm .

Table 3. Very high Reynolds numbers: Comparison of Rm_c^{Sch} for different models and DNS. The uncertainties of Rm_c are determined by the uncertainty of C_0 (Eq. 22).

	Sharp		Smooth	
	s	X_c	Rm_c^{Sch}	Rm_c
	0.33	20.5	95 ± 5	0.33
	0.39	14.5	70 ± 5	43.2
				260 ± 10
				30.2
				200 ± 10

DNS Schekochihin et al. (2007); Warnecke et al. (2023):
 $Rm_c^{Sch}_{max} \approx 350$ at $Re_\lambda = 300$
 $Rm_c \downarrow$ for higher Re
 $Rm_c^{Sch}(Re_\lambda \approx 5 \times 10^4) \gtrsim 200$

4.1. 'Sharp' model

We start with a natural and simple theoretical model proposed by Vainshtein & Kichatinov (1986), which focuses on the main features of turbulence. It describes the power-law behavior of $b(\rho)$ in the inertial range and its approximate constancy at large scales:

$$b(\rho)_{Sharp} = b_\infty \begin{cases} (\rho/\Lambda)^{1+s} & , \rho < \Lambda \\ 1 & , \rho > \Lambda \end{cases}, \quad s = 1/3 \quad (26)$$

This model was used in numerous papers (see, e.g., Rogachevskii & Kleeorin (1997); Vincenzi (2002); Boldyrev & Cattaneo (2004); Arponen & Horvai (2007); Schober et al. (2012); Kleeorin & Rogachevskii (2012); Kopyev et al. (2025)). The viscous range is not of interest for dynamo study at very large Reynolds numbers, since it is far below the magnetic diffusion scale, and cannot contribute to generation. The integral scale L used in the definition of Re, Rm is assumed to be proportional to Λ . The sharp break in (26) results in a kink in $\sigma(\rho)$, and a discontinuity in σ' . This discontinuity produces a δ -function in the potential (9). This is of course a peculiar property of the model, and just enhances and emphasizes the maximum of $U(\rho)$, but the term $\rho\sigma'$ does not play an essential role, changing the resulting Rm_c to only about 20% (Kopyev et al. 2025). Much larger contribution to Rm_c is produced by the sharp kink at the same $\rho = \Lambda$. From (25) one can see that X is the ratio of the 'end-of-the inertial-range' scale Λ and the magnetic diffusion scale r_d :

$$X = \left(\frac{b_\infty}{2\eta} \right)^{1/(1+s)} = \frac{\Lambda}{r_d} \quad \text{where} \quad r_d : b(r_d) = 2\eta$$

Kopyev et al. (2025) find that the generation threshold corresponds to the critical value of X equal to

$$X_c = 20.5$$

Then, according to (24) and (12),

$$Rm_{c(sharp)}^{Sch} = \frac{C_0}{4} X_c^{4/3} \simeq 100$$

In what follows, we will compare this result with the results of other models.

4.2. Intermittency: dependence on s

The scaling exponent of b inside the inertial range turns out to be an important parameter. It is composed of the exponents of $\langle |\delta v_\parallel|^2 \rangle$ and τ_c . Let $\langle |\delta v_\parallel|^n \rangle \propto \rho^{\zeta_n}$; then, according to the bridge

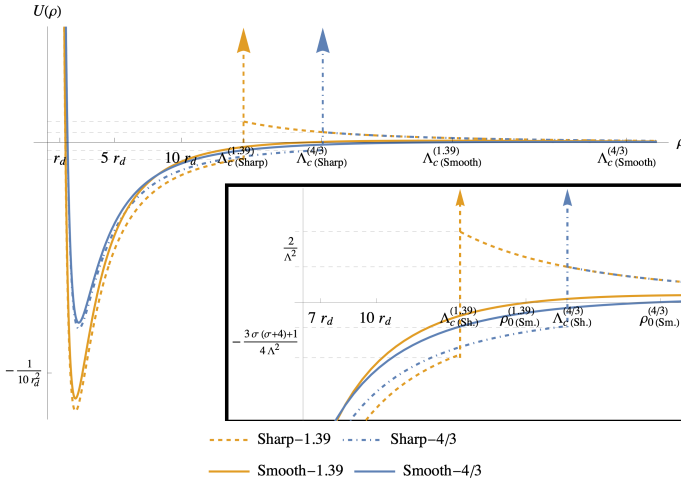


Fig. 2. Effective potential $U(\rho)$ (Eq. 9) that corresponds to the generation threshold for the two 'Sharp' and two 'Smooth' models. The length scale is normalized by the diffusion scale r_d , which is taken the same for both models. The vertical arrows correspond to the delta functions in the 'Sharp' model's potential.

relations (L'vov et al. 1997; Biferale et al. 2011), $\tau_c \propto \rho^{1-\zeta_2+\zeta_1}$ and, hence,

$$b(\rho) \propto \rho^{1+\zeta_1}. \quad (27)$$

In Kolmogorov phenomenological theory we get $s = \zeta_1 = 1/3$. However, intermittency of velocity structure functions implies that $\zeta_n > n/3$ for $n < 3$ (Frisch 1995).

The values of ζ_n depend on Re ; for very high Reynolds numbers ($Re_\lambda \gtrsim 650$) one gets $s = \zeta_1 = 0.39$ (Benzi et al. 2010; Iyer et al. 2020). Even this small change in s affects the generation properties significantly: for $s = 0.39$ we get $X_c = 14.6$, which results in smaller critical Reynolds number:

$$Pm_c \simeq \frac{2160}{Re_\lambda^2}, \quad Rm_c^{Sch} \simeq 70$$

This qualitative behavior is an important hint to explain the decrease of Rm_c for high enough Reynolds numbers. Actually, Iyer et al. (2020) showed that ζ_1 increases as a function of Re . This is a sufficient reason for the decrease of Rm_c observed by Warnecke et al. (2023).

4.3. 'Smooth' model: the effect of the transition region

Not only the inertial range but also the transition scales from inertial to integral range affect the generation for large Reynolds numbers. To demonstrate this, we consider the 'Smooth' model: it coincides with the 'Sharp' model in the inertial and integral ranges but provides more accurate description in between,

$$b(\rho)_{Smooth} = b_\infty \frac{(\rho/\Lambda)^{1+s}}{(1 + (\rho/\Lambda)^2)^{\frac{1+s}{2}}} \quad (28)$$

Since at $\rho \ll \Lambda$ and at $\rho \rightarrow \infty$ this coincides with b_{Sharp} , the definition of r_d and the relation $X = \Lambda/r_d$ remain the same. The shape of $b(\rho)$ for the 'Smooth' and 'Sharp' models is illustrated in Fig. 1.

We consider the 'Smooth' model with both 'classical' non-intermittent scaling $s = 1/3$ and more realistic $s = 0.39$. The resulting X_c and Rm_c^{Sch} are presented in Table 3.

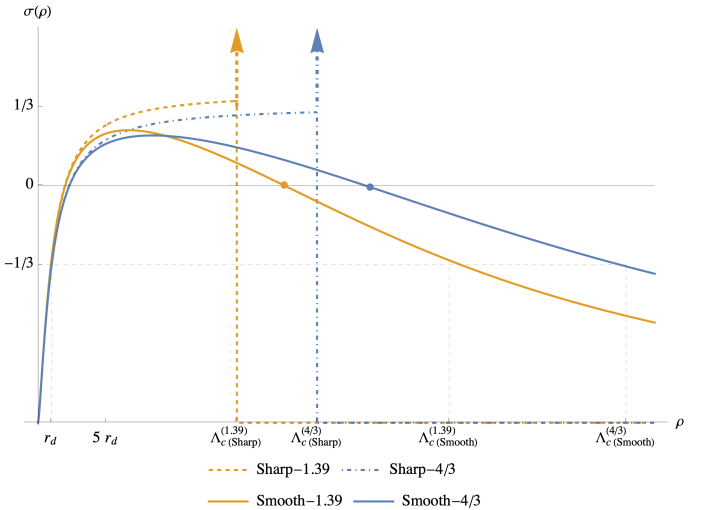


Fig. 3. Logarithmic derivative $\sigma(\rho)$, (10), for the four models. The length scale is normalized by same r_d . The parameters of each model correspond to the generation threshold.

Comparing the results of the theoretical models with the DNS data, we find that the agreement is quite reasonable. Indeed, all the models show the value of Rm_c less than the upper limit $Rm_c^{Sch} \leq 350$ found by Schekochihin et al. (2007). The data of Schekochihin et al. (2007); Iskakov et al. (2007); Warnecke et al. (2023) demonstrate the decrease of Rm_c at $Re_\lambda \gtrsim 300$, and the value of Rm_c obtained at the highest Reynolds number $Re \simeq 5 \cdot 10^4$ achieved by Warnecke et al. (2023)² is $Rm_c^{Sch} \gtrsim 200$. This agrees very well with the prediction of the Smooth model for $s = 0.39$, which is the most realistic of our models.

Comparison of the 'Smooth' and 'Sharp' models shows that the influence of the transition region is significant: the critical values of the parameters differ almost twice. What is the reason of the difference?

The velocity correlator profiles and the corresponding potentials $U(\rho)$ drawn at the critical values Λ_c are rather close in both models everywhere except for the vicinity of $\Lambda_{c(Sharp)}$: see Fig. 2. This appears to be the region where the transition zone has the most strong influence. On the other hand, this is the boundary of the region responsible for generation. Indeed, the generation threshold at any given Reynolds number corresponds to zero energy level; one can see from Fig 2 that the scales $\rho_0 : U(\rho_0) = 0$ for the Smooth models differ by less than 20% from the corresponding scales $\rho_0(Sharp) = \Lambda_{c(Sharp)}$ for Sharp models. Hence, the 'generation' region $\rho \lesssim \rho_0$ is situated for both Sharp and Smooth models within or near the scale $\Lambda_{c(Sharp)}$ and rather far from the integral scale $\Lambda_{c(Smooth)}$. Though the Sharp model is of

² The paper Warnecke et al. (2023) reports $Rm_c \approx 10^2$, but the normalization of Re and Rm that is used there is about two times lower than that of Schekochihin et al. (2007); Iskakov et al. (2007): according to Brandenburg et al. (2018), the definition of Re (and, hence, Rm) in Brandenburg et al. (2018) is probably 1.5 times smaller than those in Iskakov et al. (2007) because of different definitions of the pumping scale. On the other hand, e.g., the values of Rm_c corresponding to $Pm = 0.1$ in Brandenburg et al. (2018) and Warnecke et al. (2023) are related as 4:3. So,

$$Rm^{Sch} = Rm^{Isk} \approx \frac{3}{2} Rm^{Brand} \approx 2 Rm^W$$

course less plausible and accurate than the 'Smooth' model, it indicates better the scales that contribute most to generation. So, the difference in the values of Rm_c is probably caused by different meanings of the scale Λ in the two types of models. While $\Lambda_{c(Smooth)}$ corresponds to the integral scale of turbulence, $\Lambda_{c(Sharp)}$ acts merely as a transition range marker, which is about twice smaller scale.

The function $b(\rho)$ contributes to $U(\rho)$ by means of the logarithmic derivative $\sigma(\rho)$. So, it is interesting to compare these functions at critical regimes for different models. In Fig. 3 the functions $\sigma(\rho)$ that correspond to the generation threshold are plotted. One can see that the rising parts of the curves are almost identical, the whole difference being in the descending part of the curve. In accordance with Kazantsev (1968), the scales important for generation satisfy the condition $\sigma > 0$. Indeed, we see that, for every s , the graphs for both models intersect the line $\sigma = 0$ at $\rho \simeq \Lambda_{c(Sharp)}$. So, the Kazantsev criterion agrees well with the criterion $\rho \lesssim \rho_0$.

We see that the transition region is probably the one that determines the generation boundary. On the other hand, in the absence of the self-similarity of velocity correlators at the largest scales, the properties of this transition region may not be uniquely related to the velocity properties at the integral scales. If so, the comparison of some characteristics related to the transition region, for example ρ_0 or the scale where $\sigma = 0$, for different DNS-s or experiments, would be more effective than the comparison of large scale parameters like magnetic Reynolds numbers.

In other words, it may be more effective to describe the generation threshold by means of some combination of parameters that describe the surrounding of the point ρ_0 or $\rho : \sigma = 0$ rather than by means of integral characteristics such as Rm_c .

5. Increment near the generation threshold

Now we consider the growth rate $\gamma = \lim_{t \rightarrow \infty} d \ln G/dt$ of the magnetic field correlator near the generation threshold. Namely, we are interested in

$$g \equiv Rm \frac{d\gamma}{dRm} \Big|_{Rm=Rm_c} = \frac{d\gamma}{d \ln(Rm/Rm_c)} \Big|_{Rm=Rm_c}$$

We note that, since the expression contains the ratio Rm/Rm_c , it does not depend on the choice of normalization.

Rogachevskii & Kleerorin (1997); Kleerorin & Rogachevskii (2012) predicted this value to be constant along the critical curve ($Rm = Rm_c$) for small Prandtl numbers. The data of Warnecke et al. (2023) confirms this prediction for a wide range of Prandtl numbers beginning with $Pm \lesssim 0.1$. The value of the coefficient found by Brandenburg et al. (2018); Warnecke et al. (2023) is

$$\left(\frac{\gamma_{DNS-W}}{\ln(Rm/Rm_c)} \right)_{Pm} = 0.022 v_{rms} k_f$$

where k_f is the pumping wavenumber; taking into account the relation $\varepsilon/(v_{rms}^3 k_f) = 0.041$ given by Brandenburg et al. (2018), one can express this in terms of universal variables:

$$\left(\frac{\gamma_{DNS-W}}{\ln(Rm/Rm_c)} \right)_{Pm} = 0.18 \frac{\varepsilon}{u'^2} \quad (29)$$

To compare this coefficient with the Kazantsev theory, we are again forced to take the value $Re_\lambda = 140$, since for this

Table 4. Parameters of the simulations of Schekochihin et al. (2007) used to obtain equation (31)

Run	Rm^{Sch}	Re^{Sch}	Pm	Re_λ	γ	u'	ε
A3	110	440	0.25	111	-0.22	0.8	1
B2	220	440	0.5	110	0.49	0.8	1

Reynolds number we have information on Lagrangian statistics (Biferale et al. 2011). The Prandtl number corresponding to this Re_λ is $Pm \approx 0.3$ and does not belong to the range where the increment slope is constant. However, according to the data of Warnecke et al. (2023), the value is close to the boundary and the slope does not differ significantly.

Making use of the velocity statistics given by Biferale et al. (2011); Donzis & Sreenivasan (2010) we solve Eq. (8) numerically for values of γ close to zero, and obtain (for $Re_\lambda = 140$)

$$\left(\frac{\gamma_{th}}{\ln(Rm/Rm_c)} \right)_{Re} \simeq 1.3 \varepsilon/u'^2 \quad (30)$$

To compare it with (29), one has to note that the increment derivatives in (29) are taken at constant Prandtl numbers, while in (30) they are taken at constant Reynolds numbers. These two derivatives are related by

$$\frac{(\partial \gamma / \partial \ln Rm)_{Pm}}{(\partial \gamma / \partial \ln Rm)_{Re}} = - \frac{Re}{Pm_c} \frac{dPm_c}{dRe} = - \frac{d \ln Pm_c}{d \ln Re}$$

This follows from (13) and from the condition that $\gamma = 0$ along the critical curve $Rm_c(Re)$. From the data presented by Schekochihin et al. (2007); Warnecke et al. (2023) we find

$$- \frac{d \ln Pm_c}{d \ln Re} = \left(1 - \frac{d \ln Rm_c}{d \ln Pm} \right)^{-1} \simeq 0.5$$

The results for the theoretical calculation and for the DNS results are summarized in Table 5. We also add g obtained from the DNS data (Schekochihin et al. 2007) (see table 4):

$$\left(\frac{\gamma_{DNS-Sch}}{\ln(Rm/Rm_c)} \right)_{Re} \simeq \frac{0.49 + 0.22}{\ln(220/110)} \simeq 0.7 \frac{\varepsilon}{u'^2} \quad (31)$$

One can see that the results differ significantly. Even the results of the two numerical simulations are quite different; taking this into account, the fact that the theoretical and numerical results are of the same order is a good correspondence.

The significant difference between the theoretical and numerical results can have, e.g., following reasons:

- Data for hydrodynamics are taken from different sources, this affects the errors much. In particular, C_0 is difficult to determine and depends strongly on the isotropy of the flow and other factors. We used the value (22) found analytically (Sawford 1991) in the frame of a particular model. The difference given by various DNSs and experiments is up to 1.5 times in both directions (Lien & D'Asaro 2002).
- In Table 4 the estimate of the slope of a curve near the inflection point is taken by only two distant points, which may lead to underestimation of the slope. Besides, these two points are themselves known to some errors.
- The details of DNS, such as periodic boundary conditions, can affect the generation.
- Finally, the real slope may be smaller than the one predicted by the Kazantsev model because of the non-Gaussianity of the

Table 5. The increment slope $d\gamma/d\ln(Rm/Rm_c)$ for $Pm=\text{const}$ (g_{Pm}) and $Re=\text{const}$ (g_{Re}) obtained from the theory and the DNS

	Re_λ	g_{Pm}	g_{Re}
Warnecke et al. (2023)	$\gtrsim 100$	0.2	0.36
Schekochihin et al. (2007)	110	0.35	0.7
Theory	140	0.66	1.33

velocity flow. Taking this factor into account would decrease the slope (Kopyev et al. 2024).

In the case of large Reynolds numbers, we have not enough data for non-simultaneous velocity statistics, and have to restrict ourselves by dimensional considerations. For both Sharp and Smooth models, inside the inertial range of scales we get

$$b(\rho)|_{r_v \ll \rho \ll L} = \rho^{4/3} \left(\frac{\rho}{\Lambda} \right)^{s-1/3} \varepsilon^{1/3} \tilde{a}(Re_\lambda), \quad (32)$$

where \tilde{a} is a dimensionless parameter. As $Re \rightarrow \infty$, the function $\tilde{a}(Re_\lambda)$ has a constant limit (Frisch 1995). With account of (23), for the Sharp model from the condition $b(\Lambda) = b_\infty$ we then get

$$\Lambda = \left(\frac{b_\infty}{\varepsilon^{1/3} \tilde{a}} \right)^{3/4} = \left(\frac{4}{C_0 \tilde{a}} \right)^{3/4} \frac{u'^3}{\varepsilon}$$

For the Smooth model, the result differs no more than by a multiplier ~ 2 . Then, the increment is

$$g = \frac{c X_c^{s-1} 2\eta}{1+s} \frac{b_\infty}{r_d^2} = \frac{c}{1+s} \frac{b_\infty}{\Lambda^2} = \frac{c}{1+s} \sqrt{\frac{C_0}{4}} \frac{\varepsilon}{u'^2} \tilde{a}^{3/2}$$

This confirms that the increment does not depend on the Reynolds number for very high Re . Kleerorin & Rogachevskii (2012) obtained this result for $s = 1/3$; we prove that the presence of intermittency practically does not affect it, so the independence of g preserves up to the values of Re where the bottleneck effect is essential.

6. Discussion

So, in the paper we study the magnetic field generation in a turbulent flow near the generation threshold. We compare theoretical predictions of the extended Kazantsev theory with results of DNS for two cases: the value of the local Reynolds number $Re_\lambda = 140$, which is distinguished by presence of both magnetohydrodynamical and Lagrangian hydrodynamical data, and the limiting case of very large Reynolds numbers. To calculate the time-integrated velocity structure function $b(\rho)$ (see Eq. 4), we use the quasi-Lagrangian statistics (in particular, the Lagrangian velocity correlation time). This provides the concordance with the DNS results by orders of magnitude better than those found with the Eulerian statistics. The values of critical magnetic Reynolds and magnetic Prandtl numbers obtained from the theory and from DNS differ by no more than $\sim 10\%$.

An ideal way to compare DNS with theory should be to find $b(\rho)$ and Pm_c in the same DNS and to solve Eq.(8) with this particular $b(\rho)$. Even if neglect the term with σ' (which is difficult to calculate numerically) in the potential, one would get rather high accuracy presumably better than 20%. In this sense, the Kazantsev equation is a kind of 'bridge' connecting quasi Lagrangian turbulence to the parameters of magnetic field generation.

In absence of such combined DNS, we take the data of Biferale et al. (2011); Donzis & Sreenivasan (2010) for velocity

statistics for one particular Reynolds number and compare the result with the data of Schekochihin et al. (2007). The result is presented in Table 2; the concordance is quite good.

One more difficulty in comparing the theory and the numerical/experimental data is the use of different normalizations by different authors. This creates ambiguity and additional need to coordinate data. In order to avoid this, it would be better to provide the stability curve in terms of Pm_c as a function of Re_λ , since, unlike Rm and Re , they are independent of the pumping properties of a particular flow and universal in the sense that they can be expressed in terms of the basic parameters $\varepsilon, v_{rms}, \nu, \eta$. Another way is to use more universal definition of the integral scale. In this paper we present our results in terms of Re^{Sch}, Rm^{Sch} that are defined by (12) and (13).

The comparison of different models shows the importance of the transition region between the inertial and the integral ranges. While the 'bottleneck' transition between the viscous and inertial ranges is only important for relatively small local Reynolds numbers, this 'outer' transition range turns out to be essential for magnetic field generation at all Reynolds numbers.

For extremely large Reynolds numbers, the piecewise-power law model ('Sharp') represents well the qualitative properties of the generation but lowers the generation threshold significantly; the 'Smooth' model appears to be much more accurate, and demonstrates nice concordance with DNS. For the velocity scaling exponent found by Iyer et al. (2020), the obtained critical magnetic Reynolds number fits well the DNS results.

The comparison of the Sharp and the Smooth models helps to determine the region that is most responsible for the value of the generation threshold. It turns out to be about two times smaller than the parameter Λ of the Smooth model, which is comparable to the pumping scale. This scale belongs to the transition region from the inertial to the pumping range. It can be marked by the condition $\sigma(\rho) \approx d \ln b / d \ln \rho = 0$, or by the claim that the effective potential (9) is zero at the point.

Based on the comparison of our data for different scaling exponents, we propose the explanation of the decrease of the critical magnetic Reynolds number as a function of Re for $650 \gtrsim Re_\lambda \gtrsim 300$. The earlier explanation referred to the influence of the bottleneck; but the downward tendency of Rm_c continues also for $Pm \lesssim 0.01$ where the influence of the bottleneck is certainly negligible. We note that the critical magnetic Reynolds number depends essentially on the scaling exponent of the velocity structure function inside the inertial range. As it was shown by Iyer et al. (2020), the scaling exponent decreases as a function of Re from $1/3$ at relatively small Re to 0.39 as $Re \rightarrow \infty$. This decrease is enough to ensure the decrease of Rm_c .

We also study the dependence of the growth rate exponent of the magnetic field correlator on the magnetic Reynolds number. The results are presented in Table 5. The theoretical prediction differs 2–4 times from the numerical results, which in turn differ significantly from each other. On one hand, this is a good correspondence taking into account the technical uncertainties. On the other hand, one can suppose that the difference can be decreased by taking the non-Gaussianity of the velocity field into account. As in the case of Rm_c , the corresponding correction would change the theoretical result in the right direction.

To conclude, this work stresses importance of precise comparison of the kinematic dynamo theory with DNS. Actually, it would quantitatively verify (or refute) the key theoretical simplifications such as a delta-correlated velocity field. We obtain encouraging results in favor of the latter by an attempt of such a comparison using the existing numerical and theoretical data on turbulence. We hope that future DNSs will be able to com-

bine both kinematic dynamo and Lagrangian velocity properties, which would allow for an accurate comparison with the Kazantsev theory. The precise comparison would also allow for a quantitative assessment of the influence of non-Gaussian effects, such as dynamo suppression and changes in the magnetic energy spectrum. Successful confirmation of the theory at moderately low magnetic Prandtl numbers would provide a critical basis for extrapolation of its predictions to extreme, astrophysically significant Pm values, which are beyond current computational capabilities.

Acknowledgments. This work of AVK was supported by the Foundation for the Advancement of Theoretical Physics and Mathematics (BASIS).

References

Arponen, H. & Horvai, P. 2007, *Journ. Stat. Phys.*, 129, 205

Batchelor, G. K. 1950, *Proceedings of the Royal Society of London. Series A. Mathematical and Physical Sciences*, 201, 405

Benzi, R., Biferale, L., Fisher, R., Lamb, D. Q., & Toschi, F. 2010, *Journal of Fluid Mechanics*, 653, 221

Benzi, R., Ciliberto, S., Tripiccione, R., et al. 1993, *Physical review E*, 48, R29

Biferale, L., Calzavarini, E., & Toschi, F. 2011, *Physics of Fluids*, 23

Boldyrev, S. & Cattaneo, F. 2004, *Physical Review Letters*, 92, 144501

Brandenburg, A., Haugen, N. E. L., Li, X.-Y., & Subramanian, K. 2018, *MNRAS*, 479, 2827

Brandenburg, A., Neronov, A., & Vazza, F. 2024, *Astronomy & Astrophysics*, 687, A186

Brandenburg, A., Sokoloff, D. D., & Subramanian, K. 2012, *Space Sci. Rev.*, 169, 123

Brandenburg, A. & Subramanian, K. 2005, *Physics Reports*, 417, 1

Chertkov, M., Falkovich, G., Kolokolov, I., & Vergassola, M. 1999, *Physical review letters*, 83, 4065

Donzis, D. A. & Sreenivasan, K. R. 2010, *Journal of fluid mechanics*, 657, 171

Falkovich, G., Gawedzki, K., & Vergassola, M. 2001, *Reviews of modern Physics*, 73, 913

Frisch, U. 1995, *Turbulence: the legacy of A.N. Kolmogorov* (Cambridge university press)

Il'yn, A. S., Kopyev, A. V., Sirota, V. A., & Zybin, K. P. 2021, *Phys. Fluids*, 33

Il'yn, A. S., Kopyev, A. V., Sirota, V. A., & Zybin, K. P. 2022, *Physical Review E*, 105, 054130

Iskakov, A. B., Schekochihin, A. A., Cowley, S. C., McWilliams, J. C., & Proctor, M. R. E. 2007, *Phys. Rev. Lett.*, 98, 208501

Iyer, K. P., Sreenivasan, K. R., & Yeung, P. K. 2020, *Phys. Rev. Fluids*, 5, 054605

Jouve, L., Brun, A. S., Arlt, R., et al. 2008, *Astronomy & Astrophysics*, 483, 949

Kazantsev, A. P. 1968, *Sov. Phys. JETP*, 26, 1031

Kichatinov, L. L. 1985, *Magnetohydrodynamics*, 21, 1

Kleeorin, N. & Rogachevskii, I. 2012, *Physica Scripta*, 86, 018404

Kolmogorov, A. N. 1941, *Dokl. Akad. Nauk SSSR*, 32, 19

Kopyev, A. V., Il'yn, A. S., Sirota, V. A., & Zybin, K. P. 2022a, *Physics of Fluids*, 34

Kopyev, A. V., Il'yn, A. S., Sirota, V. A., & Zybin, K. P. 2024, *MNRAS*, 527, 1055

Kopyev, A. V., Il'yn, A. S., Sirota, V. A., & Zybin, K. P. 2026, in preparation to *Bulletin of the Lebedev Physics Institute*

Kopyev, A. V., Kiselev, A. M., Il'yn, A. S., Sirota, V. A., & Zybin, K. P. 2022b, *Astrophys. J.*, 927, 172

Kopyev, A. V., Sirota, V. A., Il'yn, A. S., & Zybin, K. P. 2025, arXiv preprint arXiv:2509.13206, under consideration in PRE

Lien, R.-C. & D'Asaro, E. A. 2002, *Physics of Fluids*, 14, 4456

L'vov, V. S., Podivilov, E., & Procaccia, I. 1997, *Phys. Rev. E*, 55, 7030

Mason, J., Malyshkin, L., Boldyrev, S., & Cattaneo, F. 2011, *The Astrophysical Journal*, 730, 86

Moisy, F., Tabeling, P., & Willaime, H. 1999, *Physical review letters*, 82, 3994

Moss, D., Kitchatinov, L. L., & Sokoloff, D. D. 2013, *Astronomy & Astrophysics*, 550, L9

Novikov, E. A. 1965, *Sov. Phys. JETP*, 20, 1290

Oseledec, V. I. 1968, *Transactions of the Moscow Mathematical Society*, 19, 197

Ouellette, N. T., Xu, H., Bourgoin, M., & Bodenschatz, E. 2006, *New Journal of Physics*, 8, 102

Rempel, M., Bhatia, T., Bellot Rubio, L., & Korpi-Lagg, M. J. 2023, *Space Sci. Rev.*, 219, 36

Rogachevskii, I. & Kleeorin, N. 1997, *Physical Review E*, 56, 417

Sawford, B. L. 1991, *Physics of Fluids A: Fluid Dynamics*, 3, 1577

Sawford, B. L. & Yeung, P.-K. 2011, *Physics of Fluids*, 23

Sawford, B. L., Yeung, P.-K., & Hackl, J. F. 2008, *Physics of Fluids*, 20, 065111

Schekochihin, A. A., Iskakov, A. B., Cowley, S. C., et al. 2007, *New J. Phys.*, 9, 300

Schober, J., Schleicher, D., Bovino, S., & Klessen, R. S. 2012, *Phys. Rev. E*, 86, 066412

Tobias, S., Cattaneo, F., & Boldyrev, S. 2012, *MHD Dynamos and Turbulence* in „Ten Chapters in Turbulence“ ed. by Davidson P.A., Kaneda, Y., & Sreenivasan K.R. (Cambridge University Press), 351–404

Vainshtein, S. I. 1980, *Sov. Phys. JETP*, 52, 1099

Vainshtein, S. I. & Kichatinov, L. L. 1986, *Journal of Fluid Mechanics*, 168, 73

Vincenzi, D. 2002, *Journal of statistical physics*, 106, 1073

Warnecke, J., Korpi-Lagg, M. J., Gent, F. A., & Rheinhardt, M. 2023, *Nat. Astronomy*, 7, 662

Zel'dovich, Y. B., Ruzmaikin, A. A., Molchanov, S. A., & Sokoloff, D. D. 1984, *Journal of Fluid Mechanics*, 144, 1

Zel'dovich, Y. B., Ruzmaikin, A. A., & Sokoloff, D. D. 1990, *The almighty chance* (World Scientific)

Zimmermann, R., Xu, H., Gasteuil, Y., et al. 2010, *Review of Scientific Instruments*, 81